**Journal of Nuclear Medicine, published on December 18, 2020 as doi:10.2967/jnumed.120.256255**

# A novel time-activity information sharing approach using nonlinear mixed models for patient-specific dosimetry with reduced imaging time points: application in SPECT/CT imaging post-$^{177}$Lu-DOTATATE

Theresa P Devasia[1], Yuni K Dewaraja[2], Kirk A Frey[2], Ka Kit Wong[2], Matthew J Schipper[1]

[1]Department of Biostatistics, [2]Radiology, University of Michigan, Ann Arbor, MI

**Corresponding Author:** Theresa P Devasia (PhD Student)

1415 Washington Heights, Ann Arbor, MI 48109

Email: tdevasia@umich.edu;

Phone: 678-232-4380

Fax: N/A

**Disclaimer:** No conflict of interests relevant to this article are reported.

**Financial Support:** This work was supported by grant R01CA240706, awarded by the National Cancer Institute, U.S.A.

**Word Count: 5584**

**Running title: Mixed model to reduce $^{177}$Lu time points**

**ABSTRACT**

Multiple time point SPECT/CT imaging for dosimetry is burdensome for patients and lacks statistical efficiency. A novel method for joint kidney time-activity estimation based on a statistical mixed model, a prior cohort of patients with complete time-activity data, and only one or two imaging points for new patients was compared to previously proposed single time point methods in virtual and clinical patient data. **Methods:** Data were available for ten patients with neuroendocrine tumors treated with Lu-177 DOTATATE and imaged up to four times between days 0 and 7 using SPECT/CT. Mixed models using one or two time points were evaluated retrospectively in the clinical cohort, using the multiple time point fit as the reference. Time-activity data for 250 virtual patients were generated using parameter values from the clinical cohort. Mixed models were fit using one (~96h) and two (4h, ~96h) time points for each virtual patient combined with complete data for the other patients in each data set. Time-integrated activities (TIAs) calculated from mixed model fits and other reduced time point methods were compared to known values. **Results**: All mixed models and single time point methods performed well overall, achieving mean bias <7% in the virtual cohort. Mixed models exhibited lower bias, greater precision, and substantially fewer outliers compared to single time point methods. For clinical patients, one and two time point mixed models resulted in more accurate TIA estimates for 94% (17/18) and 72% (13/18) of kidneys, respectively, but should be further validated in a larger cohort. In virtual patients, mixed models resulted in more than a two-fold reduction in the proportion of kidneys with |bias| > 10% (6% vs. 15%). **Conclusions:** Mixed models based on a historical cohort of patients with complete time-activity data and new patients with only one or two SPECT/CT scans demonstrate less bias on average and significantly fewer outliers when estimating kidney TIA, compared with popular reduced time point methods. Use of mixed models allows for reduction of the imaging burden while maintaining accuracy, which is crucial for clinical implementation of dosimetry-based treatment.

**Key Words: Mixed model, Lu-177 DOTATATE, radionuclide therapy, dosimetry, SPECT/CT**

With recent US Food and Drug Administration approval and ongoing clinical trials for new radionuclide therapies, there is much interest in quantitative imaging for personalized dosimetry-guided treatment. This includes Lutetium-177 (Lu-177) DOTATATE peptide receptor radionuclide therapy (PRRT) for the treatment of neuroendocrine tumors (NETs). Although approved on a fixed-activity basis (7.4 GBq/cycle times four cycles), there is much potential to personalize the treatment by exploiting the gamma-rays of Lu-177 that are suitable for SPECT/CT imaging. SPECT/CT-imaging based dosimetry following one cycle can be used to plan the subsequent cycle by safely adjusting the activity based on the renal or renal and lesion absorbed doses *(1,2)*.

Due to variability in pharmacokinetics, personalized dosimetry in radionuclide therapies typically requires sequential imaging over multiple days post-administration to determine the time-activity curve and the area under this curve, known as the time-integrated activity (TIA). Exponential functions are customarily used to fit the measured time-activity data, and two or three sampling points per exponential term and measurement period up to three to five times the effective half-life are recommended *(3)*. A number of recent studies have considered simplified personalized renal dosimetry in PRRT *(4-12)* and Lu177-PSMA therapy *(13,14)*. In particular, methods for approximating the PRRT TIA using a single activity measurement, introduced for Lu-177 DOTATATE by Hanscheid et al *(4)* and for Y-90 DOTATOC by Madsen et al *(5)*, have gained popularity. While the approach of individual curve fitting is simple, it is ad-hoc for limited sampling points and lacks statistical efficiency as it fails to exploit useful information that may exist across patients. Use of population-level kinetics for all patients may work well for an “average” patient, but for outliers, large errors are possible. An individual’s time-activity curve may be conceptualized as some deviation from a population-level curve. To personalize treatment, we aim to leverage information across patients while also accounting for individual variation. This formulation naturally lends itself to the mixed modeling approach.

Mixed models contain both fixed effects that are shared across all subjects and random effects that vary among patients. Mixed models are commonly used in pharmacokinetics *(15)*, yet application in radionuclide therapy dosimetry has been limited. Previously, our group used nonlinear mixed modeling in I-131 radioimmunotherapy to demonstrate good correlation between tracer-predicted and therapy-delivered absorbed doses *(16)*. Merrill et al *(17)* used mixed models to create virtual patient time-activity data and estimate both the TIA and optimal sampling schedule for radioiodine therapy.

To our knowledge, nonlinear mixed models with information sharing, as proposed here, have not been exploited to reduce the imaging burden in radionuclide therapy dosimetry. For Lu-177 PRRT of NETs, we construct biexponential mixed models using complete time-activity data for a historical group of patients and reduced numbers of time points (one or two) for new patients. In limited clinical data and in 500 virtual kidneys with realistic pharmacokinetics, we compare the performance of our proposed mixed models with the single time point approaches of Madsen et al and Hanscheid et al. Comparison is also made to standard monoexponential time-activity fitting with two time points.

## MATERIALS AND METHODS

### Patient Characteristics

The clinical study entailed a retrospective analysis of ten patients (Supplemental Table 1) who volunteered for multiple time point SPECT/CT imaging following one of the cycles of standard 177Lu-DOTATATE PRRT of NETs performed at the University of Michigan Medical Center between August 2018 and March 2020. The study was approved by the Institutional Review Board, and all patients provided written informed consent.

**Patient Imaging and Image Processing**

*Quantitative Imaging.* Sequential imaging at up to four time points ("full time point data") was performed on a Siemens Intevo Bold SPECT/CT system. For all patients, the first time point was prior to discharge on the day of therapy, while subsequent time points were between days 1 and 7, depending on patient and clinic schedule. An attempt was made to schedule one of these time points at ~96h considering prior reports *(4,6)* that identified this as optimal for single time point imaging-based dosimetry in similar cohorts.

SPECT reconstruction was performed within Siemens xSPECT Quant software using recommended presets *(18)*. Imaging and reconstruction parameters are indicated in Supplemental Table 1. With xSPECT Quant, image voxel values are directly available in units of Bq/mL, hence no external calibration factors were applied.

*Kidney segmentation and VOI propagation*. Left and right kidney VOIs were manually segmented slice-by-slice on the CT of the first SPECT/CT image by an experienced technologist. Following a contour intensity-based SPECT alignment procedure *(19)*, kidney VOIs were directly propagated to other time points, and time-activity data were extracted.

*Standard biexponential time-activity fit for clinical patients.* Biexponential models parameterized in equation (1) were fit to each kidney's full time-activity data. Although the truth is unknown for patients, we considered this curve and the corresponding TIA as "gold standards" when evaluating the reduced time point methods.

$$A(t_{ij}) = \frac{ke * ka}{c(ka - ke)} \times \left[exp(-ke * t_{ij}) - exp(-ka * t_{ij})\right] + \epsilon(t_{ij}) \qquad (1)$$

$$\epsilon(t_{ij}) \sim N(0, \sigma_{err}^2)$$

$$TIA = \int_0^\infty A(t)\, dt = \frac{1}{c} \qquad (2)$$

$$i = 1, \dots, n = \text{ kidney index}$$

$$j = 1, \dots, n_i = \text{ time index}$$

Here, $c$ scales the curve up or down, $ka$ ("uptake/absorption rate") and $ke$ ("elimination/clearance rate") influence the curve's shape, and $\epsilon$ is the measurement error with variance $\sigma_{err}^2$.

**Nonlinear Mixed Model Formulation**

The mixed model assumes that the parameters $ke$, $ka$, $c$ in (1) can each be expressed as a sum of fixed and random effects. Fixed effects shared across all subjects can be interpreted as population-average values. Random effects represent each subject's deviation from the mean values. The mixed model was parametrized as:

$$A(t_{ij}) = \frac{ke_i * ka_i}{c_i(ka_i - ke_i)} \times \left[exp(-ke_i * t_{ij}) - exp(-ka_i * t_{ij})\right] + \epsilon(t_{ij}) \qquad (3)$$

$$\epsilon(t_{ij}) \sim N(0, \sigma_{err}^2)$$

$$TIA_i = \frac{1}{c_i}$$

$$ka_i = \exp(\beta_1 + b_{1,i}), \quad ke_i = \exp(\beta_2 + b_{2,i}), \quad c_i = \exp(\beta_3 + b_{3,i})$$

$$b_{1,i} \sim N(0, \sigma_{ka}^2), \quad b_{2,i} \sim N(0, \sigma_{ke}^2), \quad b_{3,i} \sim N(0, \sigma_c^2)$$

$$i = 1, \dots, n = \text{ kidney index}$$

$$j = 1, \dots, n_i = \text{ time index}$$

Here, $\beta_1, \beta_2, \beta_3$ represent the fixed effects, and $b_1, b_2, b_3$ represent the random effects with variances $\sigma_{ka}^2, \sigma_{ke}^2$, and $\sigma_c^2$, respectively. We assume that $\epsilon$, $b_1$, $b_2$, and $b_3$ are mutually

independent. The model specification in (3) implicitly assumes independence between a patient's two kidneys.

Model (3) is used to fit a biexponential curve to a patient with only one or two imaging points by jointly fitting this new patient's limited measurements with full time point data for a prior cohort of patients. With this approach, once multi-time point measurements are available for a group of patients to build the mixed model, subsequent patients can be imaged with reduced time points.

**Mixed Model Fitting of Clinical Patient Time-Activity Data**

Both single time point (closest to 96h) and two time point (~4h, closest to 96h) mixed models were assessed for the clinical patients. Each patient's time-activity data were artificially reduced to these time points and combined with the full time point data for all other patients to fit model (3). **Mixed Model Fitting of Virtual Patient Time-Activity Data**

*Generating virtual patient kidney time-activity.* Known time-activity curves for 250 virtual patients (500 kidneys) were generated via a biexponential mixed model based on observed parameter values for the clinical data set. Random effects were sampled from Normal distributions and combined with their respective fixed effects to obtain the kidney-specific parameters. Such parameters were restricted to ranges slightly wider than observed clinical ranges to ensure that simulated data were reflective of the clinical data. Since kidney effective clearance for similar patient cohorts, including outliers, has been reported to be as wide as (35h, 135h) *(1,4,7,20)*, the range for $ke$ was expanded to cover these previously reported ranges. For each virtual patient, four time points ("full time point data") were selected to reflect the timing in clinical studies. Time point 1 was fixed at 4h as this is consistent across patients at our clinic, while the three other time points were allowed to vary with equal probability: time point 2 = {24h, 36h, 48h}; time point 3 = {84h, 96h, 108h}; time point 4 = {144h, 156h, 168h}. Time-activity data for

each kidney were normalized to the observed value at time point 1. Measurement error variance after normalization was set to 5% on average at each time point to reflect values reported for Lu-177 SPECT/CT quantification with state-of-the-art imaging *(18,21-22)*. This value is consistent with the measurement error used in a prior in-silico study of renal time-activity in Lu177-PSMA therapy *(23)*.

*Mixed model fitting.* For the single time point model, we selected time point 3 based on findings that identified ~96h as the optimal single time point *(4,6)*. For the two time point model, in addition to time point 3, time point 1 (4h) was selected due to the practicality of imaging before a patient is discharged on the day of therapy.

The 250 virtual patients were split into ten data sets with 25 patients each to facilitate evaluation of our proposed mixed models. For each patient in each data set, data were reduced down to time point 3 only and time points 1 and 3. Using the reduced data for that patient's kidneys in combination with the full data of the 24 other patients in the given data set, mixed models were fit and TIAs were estimated using equation (3). For the virtual patients, true time-activity curves and TIAs served as gold standards.

**Comparison of Reduced Time Point Methods**

The above single and two time point mixed models were compared to recently reported single time point methods that have been investigated for Lu-177 DOTATATE *(4-6,8)* as well as a standard monoexponential fit in the case of two time point data. The theoretical, single time point approximation of TIA proposed by Madsen et al assumes prior information is available on population kinetics, while the approximation of Hanscheid et al is based solely on the single activity measurement and the measurement time. For the Madsen method, we investigated 1) monoexponential fit with population mean effective half-life ($T_{eff}$) of 52h based on previously

reported values for similar cohorts *(4,6,7)* and 2) biexponential equation (1) approximation with population parameters estimated from the current clinical cohort.

In both clinical and virtual patient data, we compared the gold standard TIAs to TIAs estimated via: 1) biexponential mixed model using one time point; 2) biexponential mixed model using two time points; 3) monoexponential single time point Madsen method; 4) biexponential single time point Madsen method; 5) single time point Hanscheid method; 6) individual monoexponential fit based on two time points. For clinical data, the percent difference between the estimated TIA and the "gold standard" TIA was calculated. For the virtual data, the percent bias in the estimated TIA and root mean square error (RMSE) were calculated as measures of accuracy and total error, respectively *(24)*. The goodness of the curve fit was assessed visually and via Pearson's $R^2$. All model fitting was done using PROC NLMIXED in SAS version 9.4. All other analysis was done in R version 4.0.0.

## RESULTS

### Clinical Patient Results

The SPECT alignment and kidney VOI propagation for a typical patient and the corresponding kidney time-activity data are shown in Fig. 1. The biexponential individual fits for all clinical cases are shown in Fig. 2, with the complete time-activity data and fit parameters given in Supplemental Table 1. The $T_{eff}$ corresponding to $ke$ had a mean value of 59.6h (range: 35.4h-117.7h). Because of variations in patient and clinic schedules, there was large variability in all sampling times except for time point 1. For all but one case, a measurement close to 96h (± 27h) was available for our reduced time point analysis.

The reduced time point methods applied to the clinical data are compared in Table 1. The single and two time point mixed models outperform the Madsen or Hanscheid methods for

94% (17/18) and 72% (13/18) of kidneys, respectively. Full and reduced time point fitted curves for three example kidneys from the clinical cohort with fast, average, and slow clearance are compared in Fig. 3. The mixed model and monoexponential fits for the kidneys with fast (Fig. 3A) and average (Fig. 3B) clearance rates are able to approximate the shape of the “gold standard” curve quite well. However, for the kidney with slow uptake and clearance rates (Fig. 3C), none of the methods result in fits close to the “gold standard” curve. The monoexponential fit is essentially horizontal as the first and third time points have approximately equal activity values. The mixed model fits, while not close to the “gold standard” curve, better approximate its shape and TIA.

**Virtual Patient Results**

Parameter values used to generate the virtual time-activity data are in Supplemental Table 2. Simulated time-activity curves for right kidneys in one representative data set are shown in Fig. 4.

Reduced time point methods are compared in Table 2, Fig. 5, and Supplemental Figure 1. Mean bias was <7% for all methods. Densities of % bias for the mixed models are more concentrated around zero, with less mass in the tails compared to the other methods. RMSE was lowest and $R^2$ highest for the two time point mixed model. Notably, both mixed models exhibited substantially smaller proportions of kidneys with large bias, and the single time point mixed model had the narrowest range in bias. For example, 5 (1%) kidneys had mixed model |% bias| > 15% vs. 26 (5%) for Madsen and 37 (7%) for Hanscheid. The maximum magnitude of bias was 23% for mixed models, 35% for Madsen, and 36% for Hanscheid.

True curves and reduced time point fitted curves for three example virtual kidneys with fast, average, and slow clearance rates are compared in Fig. 6. The kidneys with fast (Fig. 6A) and average (Fig. 6B) clearance demonstrate that mixed model and individual monoexponential

fits can closely approximate the shape of the true activity curve. However, when uptake and clearance are slower than average (Fig. 6C), the monoexponential results in poor fit. The mixed model fits are also not as accurate as in the other two cases but are still closer to the true curves than the monoexponential.

## DISCUSSION

Statistical mixed models utilizing data from a historical cohort of patients with complete time-activity measurements and subsequent patients with one or two measurements were constructed and compared with other reduced time point methods proposed to obtain TIA for patient-specific dosimetry. All evaluated reduced time point methods performed well, with mean |bias| < 7% and <10% of cases showing |bias| > 15% in a virtual patient study with 500 kidneys (Table 1). However, mixed models substantially reduced the number of outliers, with a five-fold decrease in the number of virtual kidneys with |bias| > 15%. Mixed models almost always achieved lower bias in the clinical and virtual data and less variability, as demonstrated by the smaller RMSEs for the virtual kidneys. The mixed models effectively eliminated extreme outliers with 0/500 virtual and 0/18 clinical kidneys showing bias ≥ 25% in magnitude (Tables 1, 2).

Results from our implementations of the previous single time point methods are generally consistent with those reported by Hanscheid et al and Madsen et al. For a similar patient cohort, using the 96h time point, Hanscheid et al report that 89% (48/54) of kidneys were within 10% of the TIA from multi-time point imaging, which is consistent with our finding of 80% (398/500; Table 2). Direct comparison with the Madsen method is more difficult as their results were for Y-90 DOTATOC PRRT. However, our finding that for the current application, the 96h single time point estimate of Madsen et al is within 10% of the true estimate for 83-85% (>415/500) of kidneys (Table 2) is in line with their reported value of 70% at the optimal

sampling time of 48h derived for Y-90 DOTATOC. In general, bias in TIA estimation increases as $ka$ and $ke$ move away from their average values, as seen in the heat maps of absolute bias for the virtual patients (Fig. 7, Supplemental Figure 2). Hanscheid et al state that in order for their approximation to achieve <10% error, the single time point used must be within $(0.75T_{eff}, 2.5T_{eff})$. For a monoexponential, using 96h as the single time point, this range is equivalent to $ke$ between ($0.005h^{-1}$, $0.018h^{-1}$). This is consistent with our heat maps for the Hanscheid and Madsen methods, where the largest errors were for high $ke$ values up to $0.022h^{-1}$. Note that $ke$ values below $0.005h^{-1}$ were not observed in the simulations. Mixed models can be viewed through the empirical Bayes framework. Parameter estimates are then "shrinkage" estimators, meaning that outlier patients and patients with noisy data are drawn closer to the population average than patients whose time-activity curves are more typical or are less noisy. The resulting TIAs may exhibit some small bias but also reduced variance, and thus reduced probability of large bias (Fig. 5). Our clinical analysis was limited by its small sample size, but as more data become available, the results, including outliers (Fig. 4C), should mirror those of the virtual study.

A limitation of the current study is that we opted to investigate a single measurement at 96h based on prior reports *(4,6).* In addition, we chose 4h as the second time point for patient convenience as it enables imaging before discharge on the day of therapy. For the single time point, Hanscheid et al discuss the adequacy of an earlier sampling point at 72h for kidneys where the median effective half life was 51h, but recommend a later single time point such as 96h or 120h if considering liver, spleen, and NETs that tend to have longer effective half-lives; reported median effective half life was 67h, 68h, and 77 h, respectively. The theoretical optimal sampling time derived by Madsen et al was $1.44T_{eff}$, which for Lu-177 DOTATATE is closest to 72h for kidney and 120h for tumor considering the median $T_{eff}$ values reported by Hanscheid et al. Since we aim to pursue mixed modeling for tumor data in the future, we selected 96h as a

compromise, expecting that it would perform well for both kidney and tumor data. This is consistent with the recommendations of Hanscheid et al and Sundlov et al. For the two time point mixed model, there is potential to consider other combinations of time points that may lead to more accurate estimation of TIA, and others have explored such combinations further, for example in Lu-177 PSMA therapy *(13)*. In our analysis, the single time point mixed model often performed better than the two time point mixed model, suggesting that addition of the early measurement may not be necessary. A prior study also suggests that inclusion of a premature activity measure may lead to biased TIA estimates *(15)*. However, inclusion of the initial time point may lead to a better curve fit ($R^2$ > 0.93 vs. > 0.82 in Table 2) compared to using only the ~96h time point. Accurate estimation of the time-activity curve shape can have implications when estimating biological effective dose (BED) where dose rate effects are considered.

Our mixed models were fit assuming kidneys from the same patient and all random effects are independent. Exploring correlation among both kidneys within a patient and among the random effects is an avenue of future work. A potential limitation of our mixed model is the assumption that a historical cohort with multiple time point Lu-177 SPECT/CT is available, which may not be a reality for many clinics. However, post-treatment SPECT/CT imaging is becoming more accessible with recent updates in reimbursement policies. Furthermore, data sharing across centers, such as the information provided in Supplemental Table 1 and images we have deposited in the University of Michigan Library Data Sharing repository *(25)*, can facilitate model building.

While the mixed model demonstrated good performance in our limited clinical cohort and simulations based on this cohort, we expect to validate these results with a larger clinical data set. With more data, there is also the potential to examine the mixed model's performance in patient subgroups. For example, separate mixed models could be built based on clinical factors (e.g. estimated glomerular filtration rate, Supplemental Table 1) known to influence kidney

pharmacokinetics to further improve fit. Although we limited our investigation to kidney dosimetry following PRRT, it is also possible to extend this method to other therapies and organs. However, validation studies such as the one performed here should be carried out for each application prior to routine clinic use. The most natural extension of our study would be to apply this method to estimating time-activity curves for tumor dosimetry in Lu-177 DOTATATE, and such work in ongoing.

## CONCLUSION

This study demonstrates that a mixed model can effectively share time-activity information across patients to improve TIA estimation for patient-specific renal dosimetry relative to other reduced time point methods. This novel approach that relies on a historical cohort with complete time-activity data and new patients with one or two SPECT/CT imaging points resulted in less bias, greater precision, and more than two-fold and five-fold reductions in the number of outliers with bias >10% and >15%, respectively.

**DISCLOSURE:** No conflict of interest relevant to this article is reported. This work was supported by grant R01CA240706, awarded by the National Cancer Institute, U.S.A.

## Key Points

**QUESTION:** Can a statistical mixed model based on a historical cohort with complete time-activity data and future patients imaged only at one or two time points produce accurate time-integrated activity (TIA) estimates for renal dosimetry of patients with neuroendocrine tumors treated with Lu-177 DOTATATE?

**PERTINENT FINDINGS:** The mixed models demonstrated better accuracy and precision in estimating TIA for dosimetry compared to previous reduced time point methods that have been

investigated for Lu-177 PRRT. Most notably, in a virtual study with 500 kidneys, the mixed model reduced the number of outliers with absolute bias in TIA > 10% by more than a factor of 2. In the clinical study, the single time point mixed model demonstrated better performance than alternative single time point methods in 94% (17/18) of kidneys.

**IMPLICATIONS FOR PATIENT CARE:** Clinics with access to historical patient time-activity data may reduce imaging for future patients to one or two time points when performing patient-specific dosimetry. Practical methods that ease the imaging burden to patients and clinics will facilitate clinical implementation of dosimetry-guided radionuclide therapy, which is key to reducing the potential for over- or under-treating patients.

## REFERENCES


1. Sundlov A, Sjogreen-Gleisner K, Svensson J, et al. Individualised 177Lu-DOTATATE treatment of neuroendocrine tumours based on kidney dosimetry. *Eur J Nucl Med Mol Imaging*. 2017;44:1480-1489.
2. Sandström M, Garske-Román U, Johansson S, Granberg D, Sundin A, Freedman N. Kidney dosimetry during $^{177}$Lu-DOTATATE therapy in patients with neuroendocrine tumors: aspects on calculation and tolerance. *Acta Oncol*. 2018;57:516-521
3. Siegel JA, Thomas SR, Stubbs JB, et al. MIRD pamphlet no. 16: Techniques for quantitative radiopharmaceutical biodistribution data acquisition and analysis for use in human radiation dose estimates. *J Nucl Med*. 1999;40:37S-61S
4. Hänscheid H, Lapa C, Buck AK, Lassmann M, Werner RA. Dose mapping after endoradiotherapy with $^{177}$Lu-DOTATATE/DOTATOC by a single measurement after 4 days. *J Nucl Med*. 2018;59:75-81.
5. Madsen MT, Menda Y, O'Dorisio TM, O'Dorisio MS. Technical Note: Single time point dose estimate for exponential clearance. *Med Phys*. 2018;45:2318-2324.
6. Sundlöv A, Gustafsson J, Brolin G, et al. Feasibility of simplifying renal dosimetry in $^{177}$Lu peptide receptor radionuclide therapy. *EJNMMI Phys*. 2018;5:12.
7. Willowson KP, Eslick E, Ryu H, Poon A, Bernard EJ, Bailey DL. Feasibility and accuracy of single time point imaging for renal dosimetry following $^{177}$Lu-DOTATATE ('Lutate') therapy. *EJNMMI Phys*. 2018;5:33.
8. Zhao W, Esquinas PL, Frezza A, Hou X, Beauregard JM, Celler A. Accuracy of kidney dosimetry performed using simplified time activity curve modelling methods: a $^{177}$Lu-DOTATATE patient study. *Phys Med Biol*. 2019;64:175006.

9. Guerriero F, Ferrari ME, Botta F, et al. Kidney dosimetry in $^{177}$Lu and $^{90}$Y peptide receptor radionuclide therapy: influence of image timing, time-activity integration method, and risk factors. *Biomed Res Int*. 2013;2013:935351.
10. Heikkonen J, Mäenpää H, Hippeläinen E, Reijonen V, Tenhunen M. Effect of calculation method on kidney dosimetry in $^{177}$Lu-octreotate treatment. *Acta Oncol*. 2016;55:1069-1076.
11. Del Prete M, Arsenault F, Saighi N, et al. Accuracy and reproducibility of simplified QSPECT dosimetry for personalized $^{177}$Lu-octreotate PRRT. *EJNMMI Phys*. 2018;5:25.
12. Delker A, Ilhan H, Zach C, et al. The Influence of Early Measurements Onto the Estimated Kidney Dose in [(177)Lu][DOTA(0),Tyr(3)]Octreotate Peptide Receptor Radiotherapy of Neuroendocrine Tumors. *Mol Imaging Biol*. 2015;17:726-734
13. Rinscheid A, Kletting P, Eiber M, Beer AJ, Glatting G. Influence of sampling schedules on [$^{177}$Lu]Lu-PSMA dosimetry. *EJNMMI Phys.* 2020;7.
14. Jackson PA, Hofman MS, Hicks RJ, Scalzo M, Violet JA. Radiation Dosimetry in $^{177}$Lu-PSMA-617 Therapy Using a Single Post-treatment SPECT/CT: A Novel Methodology to Generate Time- and Tissue-specific Dose Factors. *J Nucl Med*. 2020;61:1030-1036.
15. Davidian M, Giltinan DM. Nonlinear Models for Repeated Measure Data. New York, NY: Chapman and Hall; 1995.
16. Schipper MJ, Koral KF, Avram AM, Kaminski MS, Dewaraja YK. Prediction of therapy tumor-absorbed dose estimates in I-131 radioimmunotherapy using tracer data via a mixed-model fit to time activity. *Cancer Biother Radiopharm*. 2012;27:403-411.
17. Merrill S, Horowitz J, Traino AC, Chipkin SR, Hollot CV, Chait Y. Accuracy and optimal timing of activity measurements in estimating the absorbed dose of radioiodine in the treatment of Graves' disease. *Phys Med Biol*. 2011;56:557-571.
18. Tran-Gia J, Lassmann M. Characterization of Noise and Resolution for Quantitative $^{177}$Lu SPECT/CT with xSPECT Quant. *J Nucl Med*. 2019;60:50-59.

19. Mirando D, Dewaraja, YK, Cole NM, Nelson AS. In pursuit of fully automated dosimetry: evaluation of an automatic VOI propagation algorithm using contour intensity-based SPECT alignment. *Eur J Nucl Med Mol Imaging*. 2020;47(Suppl 1): S236.
20. Schuchardt C, Kulkarni H, Zachert C, Baum RP. Dosimetry in Targeted Radionuclide Therapy: the Bad Berka Dose Protocol-Practical Experience. *JPMER*. 2013;47:65-73.
21. Ljungberg M, Celler A, Konijnenberg MW, et al. MIRD Pamphlet No. 26: Joint EANM/MIRD Guidelines for Quantitative 177Lu SPECT Applied for Dosimetry of Radiopharmaceutical Therapy. *J Nucl Med*. 2016;57:151-162
22. Gustafsson J, Brolin G, Cox M, Ljungberg M, Johansson L, Sj€ogreen Gleisner K. Uncertainty propagation for SPECT/CT-based renal dosime- try in 177Lu peptide receptor radionuclide therapy. *Phys Med Biol*. 2015;60:8329.
23. Rinscheid A, Kletting P, Eiber M, Beer AJ, Glatting G. Technical Note: Optimal sampling schedules for kidney dosimetry based on the hybrid planar/SPECT method in $^{177}$ Lu-PSMA therapy. *Med Phys*. 2019;46:5861-5866.
24. Casella G, Berger RL. *Statistical Inference*. Belmont, CA: Duxbury; 1990: 330.
25. Radionuclide PET/CT, SPECT/CT, and Contours Collection. University of Michigan Deep Blue Data Repository website. Available from: https://deepblue.lib.umich.edu/data. Accessed September 1, 2020.

TABLE 1. Performance of the reduced time point (TP) methods for clinical cohort. Patient 5 was excluded from analysis due to not having a ~96h measurement. $\%\ \text{Difference} = 100 * \frac{\text{TIA}_{\text{Estimated}} - \text{TIA}_{\text{Gold Standard}}}{\text{TIA}_{\text{Gold Standard}}}$. MM = mixed model. "Mono" and "Bi" refer to monoexponential and biexponential, respectively.

| | | % Difference in TIA [$R^2$ of curve fit] | | | | | |
|---|---|---|---|---|---|---|---|
| **Patient** | **Kidney** | **Mono 1 TP Madsen** | **Bi 1 TP Madsen** | **1 TP Hanscheid*** | **1 TP MM** | **2 TP MM** | **2 TP Mono** |
| **1** | Left | 4.1 [0.88] | -3.1 [0.99] | -3.0 | -1.7 [0.99] | -2.4 [0.99] | -3.1 [0.89] |
| | Right | 2.1 [0.88] | -5.0 [0.99] | -4.9 | -3.0 [0.99] | -3.1 [0.99] | -4.0 [0.89] |
| **2** | Left | 0.7 [0.89] | -4.0 [0.99] | 1.8 | -2.7 0.99] | -0.9 [0.99] | -1.1 [0.90] |
| | Right | 0.9 [0.89] | -3.8 [0.99] | 2.0 | -2.5 [0.99] | -0.7 [0.99] | -0.9 [0.90] |
| **3** | Left | 1.5 [0.93] | -3.3 [0.96] | 2.3 | -1.8 [0.97] | 5.5 [0.98] | 5.4 [0.93] |
| | Right | -18.4 [0.92] | -22.3 [0.93] | -17.7 | -15.9 [0.95] | 4.7 [0.98] | 2.6 [0.93] |
| **4** | Left | -6.2 [0.93] | -10.3 [0.96] | -4.3 | -7.3 [0.97] | -0.5 [0.98] | -1.7 [0.93] |
| | Right | -6.9 [0.93] | -11.0 [0.96] | -5.1 | -8.0 [0.97] | -1.2 [0.98] | -2.4 [0.93] |
| **6** | Left | 0.3 [0.82] | -4.2 [0.97] | 1.7 | -4.4 [0.95] | -6.1 [0.96] | -4.1 [0.85] |
| | Right | 2.0 [0.81] | -2.6 [0.97] | 3.4 | -3.0 [0.95] | -4.9 [0.97] | -1.9 [0.84] |
| **7** | Left | 4.7 [0.90] | 0.2 [0.98] | 6.8 | 0.5 [0.98] | -1.4 [0.99] | 0.7 [0.92] |
| | Right | 5.8 [0.87] | 1.2 [0.99] | 7.9 | 1.2 [0.99] | -1.2 [0.99] | 2.3 [0.90] |
| **8** | Left | 0.7 [0.91] | -6.6 [0.99] | -7.7 | -0.5 [0.99] | 2.8 [0.99] | -0.1 [0.91] |
| | Right | -1.4 [0.91] | -8.5 [0.99] | -9.6 | -1.3 [0.99] | 2.6 [0.99] | -0.6 [0.91] |
| **9** | Left | 9.2 [0.86] | 1.2 [0.99] | 0.0 | 1.1 [0.99] | -2.6 [0.99] | -3.0 [0.88] |
| | Right | 15.1 [0.84] | 6.7 [0.99] | 5.4 | 4.2 [0.99] | -1.3 [0.98] | -0.5 [0.87] |
| **10** | Left | 1.2 [0.64] | -3.1 [0.86] | 3.3 | -2.8 [0.84] | -11.1 [0.98] | 310.7 [0.77] |
| | Right | -4.9 [0.62] | -9.0 [0.86] | -2.9 | -8.7 [0.84] | -16.5 [0.97] | 278.0 [0.76] |

*Hanscheid approximation provides TIA and not a curve fit.

TABLE 2. Comparison of reduced time point (TP) methods for virtual cohort (500 kidneys). $\%\ \text{Bias} = 100 * \frac{\text{TIA}_{\text{estimated}} - \text{TIA}_{\text{true}}}{\text{TIA}_{\text{true}}}$ and $\text{RMSE} = \sqrt{\frac{1}{500}\sum_{i=1}^{500}(TIA_{estimated} - TIA_{true})^2}$. MM = mixed model. "Mono" and "Bi" refer to monoexponential and biexponential, respectively.

| **Metric** | **Mono 1 TP Madsen** | **Bi 1 TP Madsen** | **1 TP Hanscheid** | **1 TP MM** | **2 TP MM** | **2 TP Mono** |
|---|---|---|---|---|---|---|
| **Mean % Bias [Min, Max]** | 0.7 [-35.1, 17.5] | -3.0 [-38.2, 11.9] | 2.7 [-36.1, 18.5] | -1.9 [-19.2, 10.7] | -1.2 [-23.0, 10.1] | 6.3 [-12.8, 1061.9] |
| **# (%) Kidneys with \|Bias\| > 10%** | 85 (17.0) | 73 (14.6) | 102 (20.4) | 32 (6.4) | 15 (3.0) | 70 (14.0) |
| **# (%) Kidneys with \|Bias\| > 15%** | 26 (5.2) | 36 (7.2) | 37 (7.4) | 5 (1.0) | 2 (0.4) | 41 (8.2) |
| **# (%) Kidneys with \|Bias\| > 20%** | 10 (2.0) | 18 (3.6) | 10 (2.0) | 0 (0.0) | 1 (0.2) | 31 (6.2) |
| **# (%) Kidneys with \|Bias\| > 25%** | 6 (1.2) | 8 (1.6) | 8 (1.6) | 0 (0.0) | 0 (0.0) | 21 (4.2) |
| **RMSE** | 0.09 | 0.09 | 0.09 | 0.06 | 0.05 | 0.43 |
| **Mean $R^2$ of curve fit [Min, Max]** | 0.87 [0.59, 0.93] | 0.98 [0.82, 0.99] | ---* | 0.98 [0.82, 0.99] | 0.99 [0.93, 0.99] | 0.89 [0.74, 0.93] |

*Hanscheid approximation provides TIA and not a curve fit.

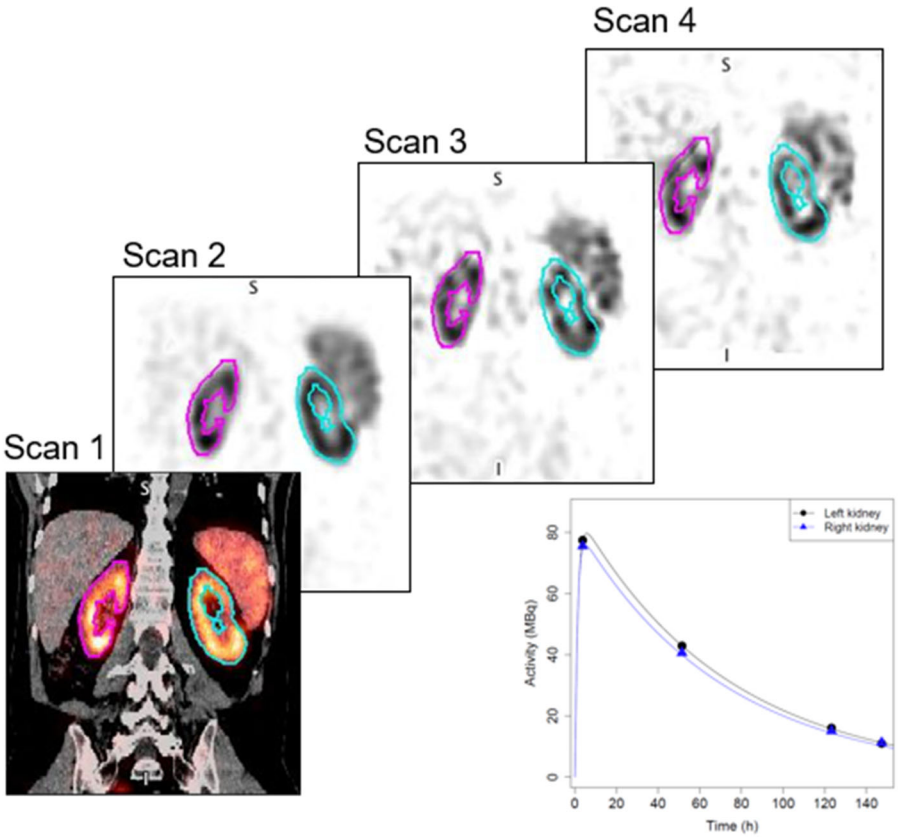


FIGURE 1. Example (clinical patient 8) SPECT/CT images with contour guided registration showing propagation of contours defined on scan 1 CT and corresponding time-activity with biexponential fit to all time points. Images have been normalized to the maximum value in each image.

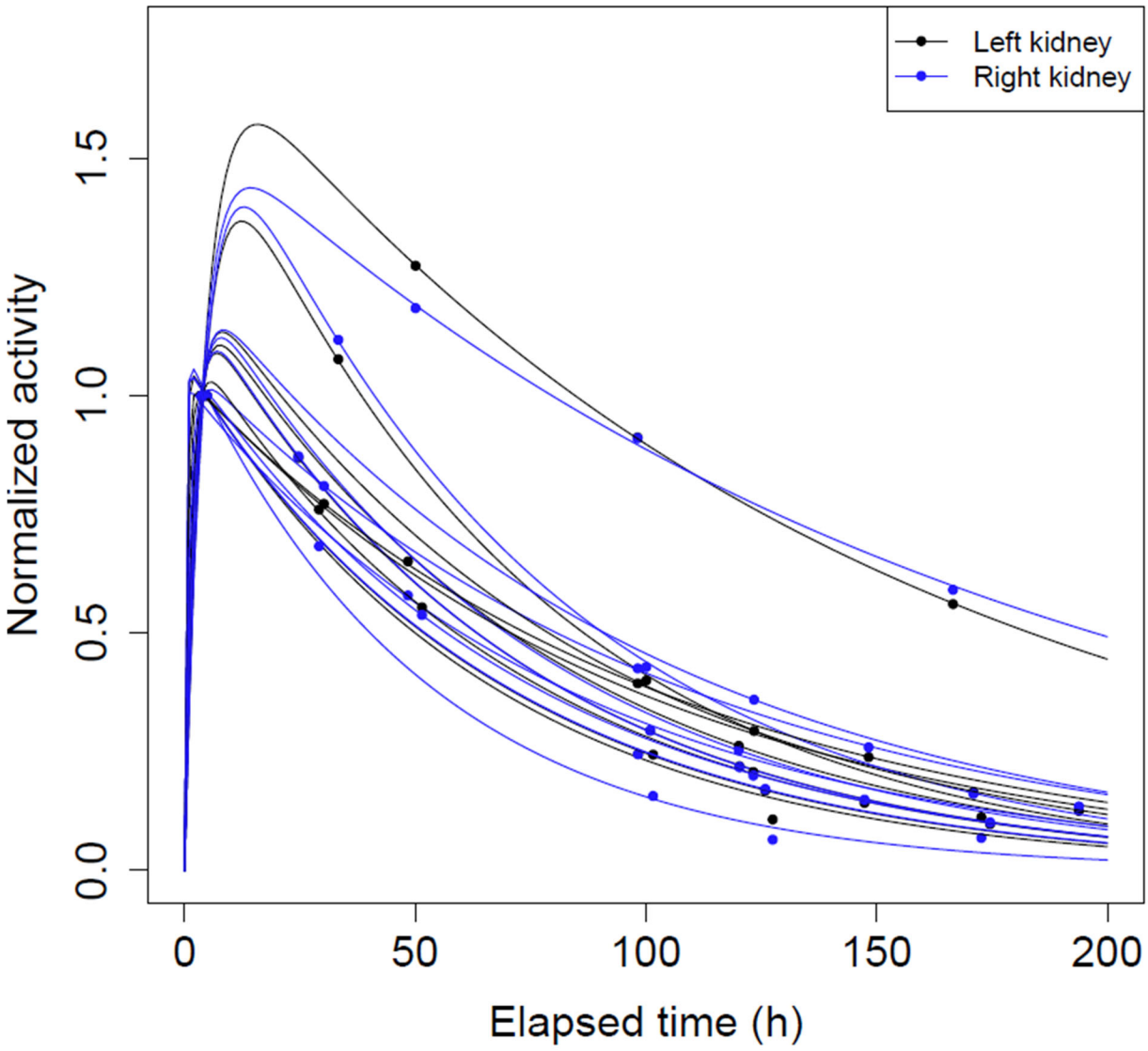


FIGURE 2. Plot of biexponential time-activity curves and observed data normalized to activity value at first measured time point for all kidneys in clinical patient data.

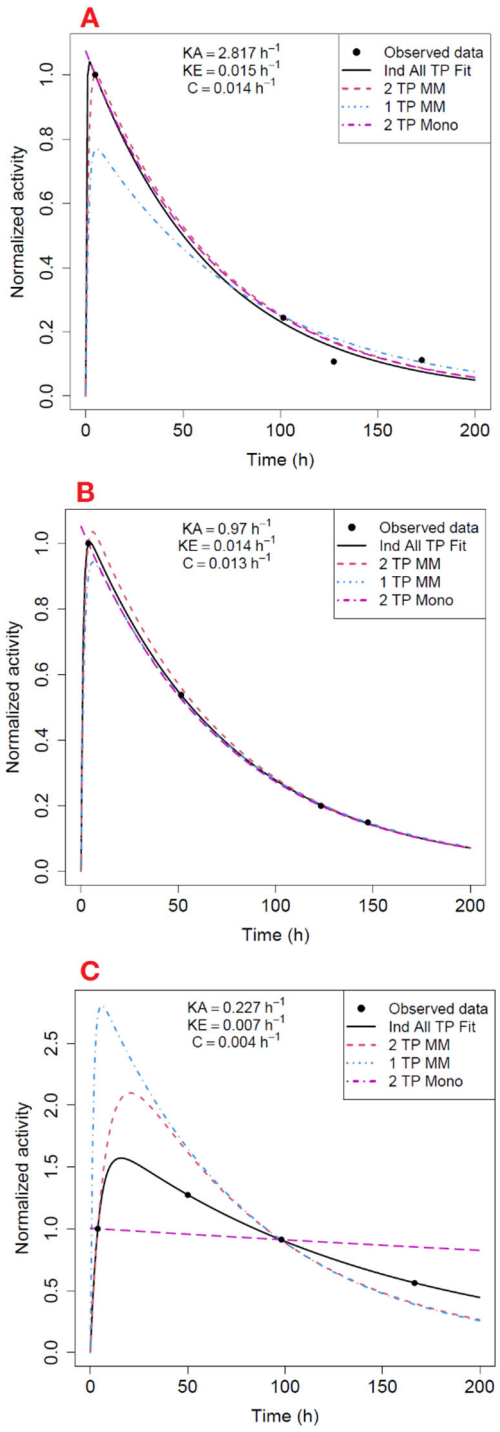


FIGURE 3. Reduced time point (TP) fits for (A) patient 3: fast clearance rate (high *ke*); (B) patient 8: typical clearance rate (average *ke*); (C) patient 10: slow clearance rate (low *ke*) kidneys in clinical cohort. “Ind” refers to biexponential fit to individual kidney’s time-activity data. MM = mixed model. “Mono” refers to monoexponential fit.

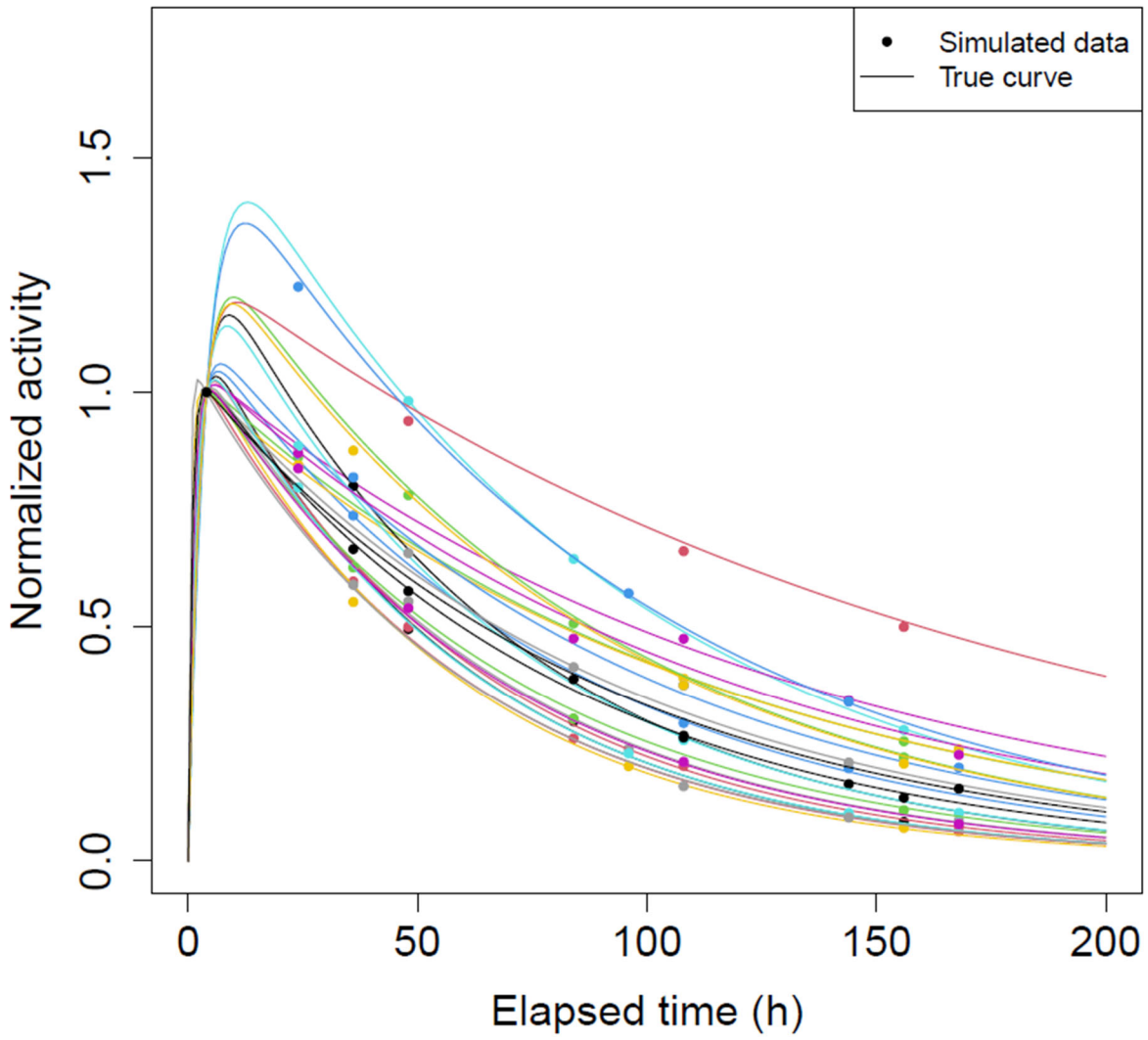


FIGURE 4. Plot of true time-activity curves and generated four time point data normalized to activity value at 4h for all 25 right kidneys in one randomly selected virtual patient data set.

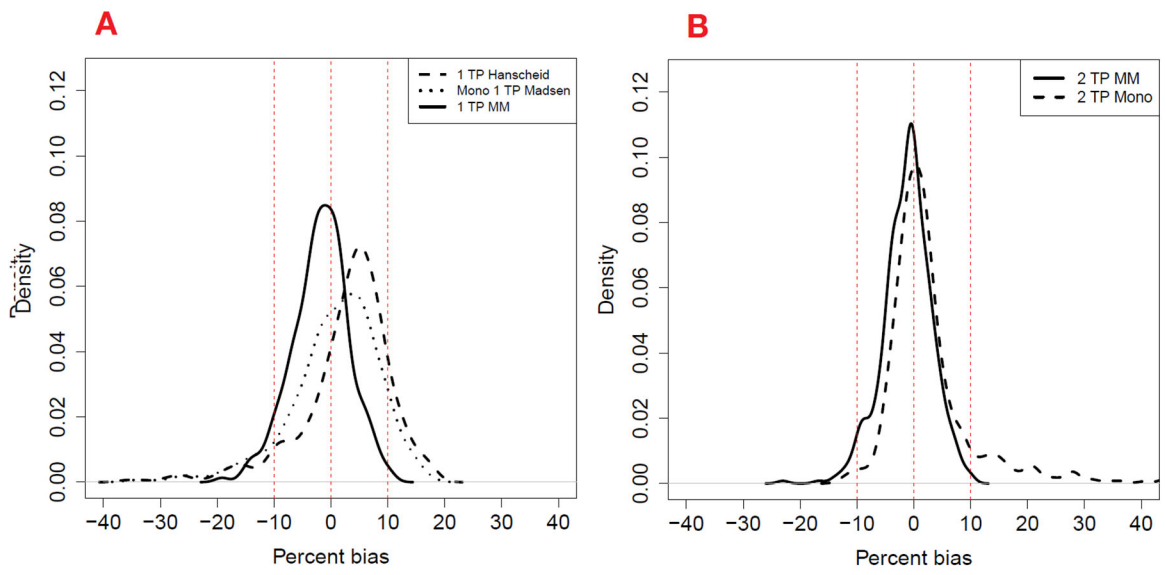


FIGURE 5. Comparison of % bias in TIA for reduced time point (TP) methods in virtual cohort of 500 kidneys for (A) one time point methods and (B) two time point methods. MM = mixed model. “Mono” refers to monoexponential fit. One kidney with two time point monoexponential % bias > 1000 not included in (B) for visualization purposes.

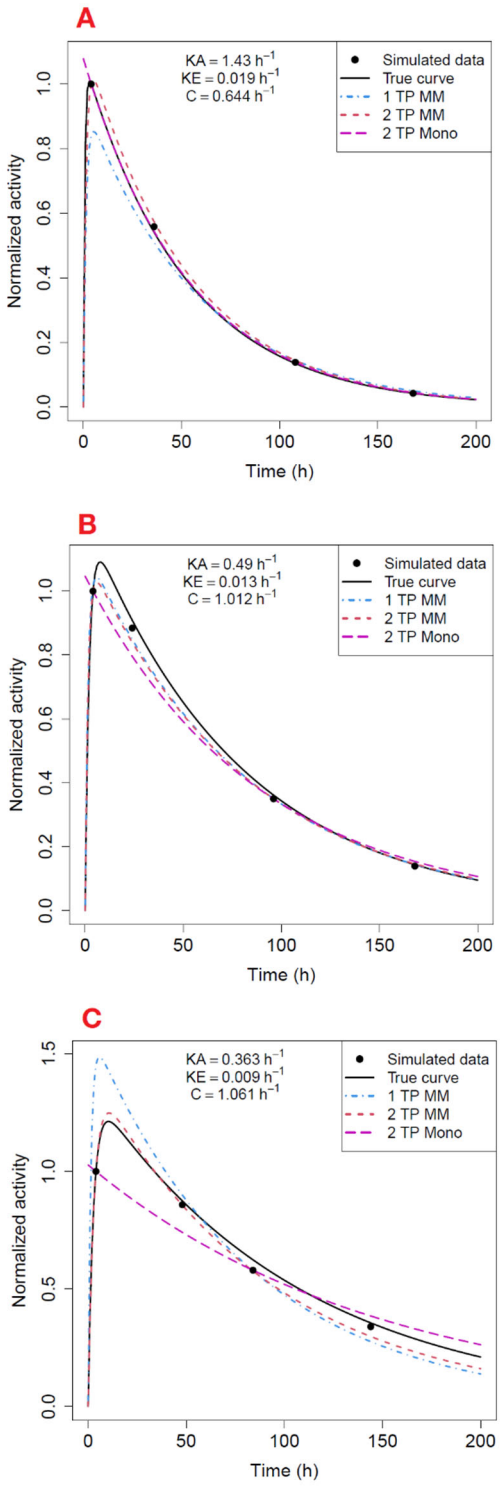


FIGURE 6. Reduced time point (TP) curve fits for example virtual kidneys with (A) fast clearance rate (high *ke*); (B) typical clearance rate (average *ke*); (C) slow clearance rate (low *ke*). MM = mixed model. “Mono” refers to monoexponential fit.

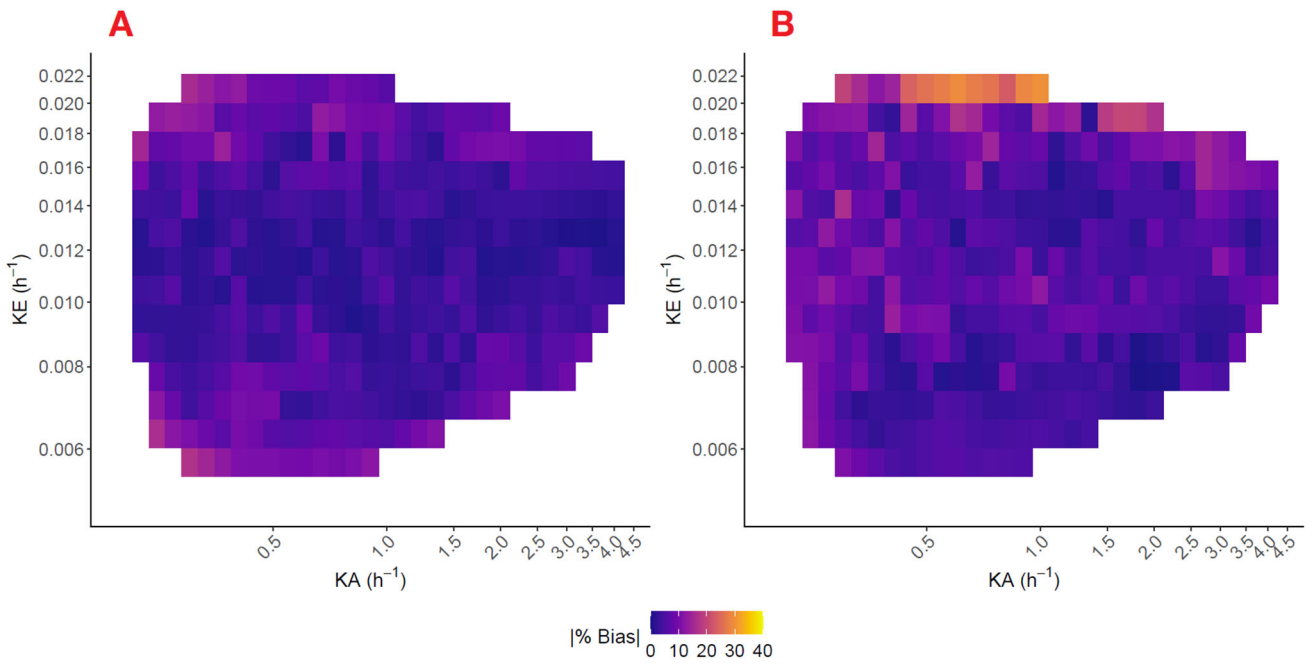


FIGURE 7. Heat maps of |% bias| vs. biexponential parameters in 500 virtual kidneys for (A) single time point mixed model and (B) Hanscheid method. White space indicates regions where no kidneys with a specific combination of parameters were simulated.

Supplemental Table 1. Patient characteristics and time-activity data for clinical patients. Data correspond to treatment cycle 1, except for patients 3 and 9, who were imaged after cycle 2. Bolded time points are used for single and two time point methods. Times are measured from the start of Lu-177 DOTATATE administration. Kidney is either left ("L") or right ("R"). $ka, ke, c$ are from individual biexponential models fit to time-activity data normalized to first activity measure. SPECT imaging parameters: Medium energy collimator, 1.5 cm crystal, 256 x 256 matrix, 60 views/head, 30 sec/view, 20% main window at 208 keV and adjacent 10% scatter windows. SPECT reconstruction was performed within Siemens xSPECT Quant using: 48 iterations 1 subset, resolution recovery, attenuation correction, triple energy window scatter correction and a 256 x 256 matrix of voxel size 2 $mm^3$. No post-reconstruction smoothing was used. The CT imaging was performed with free breathing in low-dose mode (120 kVp, 80 mAs at the first time point and 15mAs at subsequent time points). The CT matrix size was 512 x 512 x 130 with a voxel size of 0.97 x 0.97 x 3 $mm^3$.

| **Patient** | **Age** | **Sex** | **Baseline Kidney Status** | | **Injected Activity (GBq)** | **Elapsed Times (h)** | **Kidney: Activity Measurements (MBq)** | **Biexponential fit parameters** | | |
|---|---|---|---|---|---|---|---|---|---|---|
| | | | **Creatinine* mg/dL** | **EGFR† mL/min** | | | | $ka\ (h^{-1})$ | $ke\ (h^{-1})$ | $c\ (h^{-1})$ |
| **1** | 42 | M | 0.96 | >60 | 7.02 | [**3.8, 120.1**] | **L:** [83.2 ,21.1]<br>**R:** [83.3, 22.0] | **L:** 0.488<br>**R:** 0.460 | **L:** 0.013<br>**R:** 0.014 | **L:** 0.011<br>**R:** 0.011 |
| **2** | 69 | M | 0.94 | >60 | 7.15 | [**3.7**, 24.7, **101.0**, 120.3] | **L:** [77.7 ,67.8, 22.9, 16.9]<br>**R:** [65.4, 56.8, 19.2, 14.3] | **L:** 0.535<br>**R:** 0.526 | **L:** 0.014<br>**R:** 0.014 | **L:** 0.012<br>**R:** 0.012 |
| **3** | 57 | M | 0.67 | >60 | 7.33 | [**4.9, 101.6**, 127.5, 172.7] | **L:** [135.1, 21.2, 8.8, 9.2]<br>**R:** [83.0, 20.2, 8.9, 9.3] | **L:** 2.817<br>**R:** 3.173 | **L:** 0.015<br>**R:** 0.020 | **L:** 0.014<br>**R:** 0.018 |
| **4** | 64 | M | 0.98 | >60 | 7.14 | [**4.7, 98.3**, 125.9, 174.6] | **L:** [96.6, 23.6, 16.6, 9.8]<br>**R:** [104.6, 25.6, 17.6, 10.2] | **L:** 3.684<br>**R:** 3.855 | **L:** 0.015<br>**R:** 0.015 | **L:** 0.014<br>**R:** 0.014 |
| **5** | 71 | F | 0.59 | ≥90 | 7.34 | [4.4, 29.2, 48.4, 171.0] | **L:** [58.7, 40.1, 34.0, 9.5]<br>**R:** [57.6, 43.8, 37.5, 9.5] | **L:** 1.330<br>**R:** 4.658 | **L:** 0.010<br>**R:** 0.012 | **L:** 0.010<br>**R:** 0.012 |
| **6** | 62 | F | 1.17 | 47 | 7.34 | [**4.1**, 33.3, **100.1**, 193.9] | **L:** [113.2, 126.5, 48.5 ,15.2]<br>**R:** [43.4, 46.8, 17.4, 5.4] | **L:** 0.244<br>**R:** 0.234 | **L:** 0.014<br>**R:** 0.014 | **L:** 0.009<br>**R:** 0.008 |
| **7** | 38 | F | 0.99 | >60 | 7.49 | [**4.1**, 30.2, **98.2**, 148.3] | **L:** [45.8, 37.1, 19.5, 11.9]<br>**R:** [40.8, 31.5, 16.1, 9.7] | **L:** 1.925<br>**R:** 0.802 | **L:** 0.010<br>**R:** 0.010 | **L:** 0.010<br>**R:** 0.009 |
| **8** | 56 | M | 0.93 | 91 | 7.08 | [**3.8,** 51.5, **123.3**, 147.4] | **L:** [75.6, 40.7, 15.1, 11.3]<br>**R:** [77.5, 42.9 ,16.1, 11.0] | **L:** 0.713<br>**R:** 0.970 | **L:** 0.014<br>**R:** 0.014 | **L:** 0.013<br>**R:** 0.013 |
| **9** | 67 | M | 0.8 | >60 | 7.06 | [**3.8, 123.4**] | **L:** [77.1, 27.7]<br>**R:** [73.7, 21.7] | **L:** 0.462<br>**R:** 0.467 | **L:** 0.012<br>**R:** 0.010 | **L:** 0.010<br>**R:** 0.008 |
| **10** | 65 | F | 1.66 | 32 | 3.7 | [**3.8**, 50.1, **98.2**, 166.6] | **L:** [26.4, 31.3, 24.1, 15.6]<br>**R:** [26.0, 33.1, 23.7, 14.6] | **L:** 0.227<br>**R:** 0.275 | **L:** 0.007<br>**R:** 0.006 | **L:** 0.004<br>**R:** 0.004 |

*Normal creatinine level: 0.70-1.30 mg/dL; †EGFR = estimated glomerular filtration rate. Normal EGFR > 59 mL/min.

Supplemental Table 2. Parameter values used to generate virtual patient time-activity curves.

| Parameter | Simulation Value | Simulation Range |
|---|---|---|
| $ka_{fixed}$ ($h^{-1}$) | 0.667 | [0.200, 4.600] |
| $ke_{fixed}$ ($h^{-1}$) | 0.012 | [0.005, 0.022] |
| $c_{fixed}$ ($MBq^{-1}h^{-1}$) | 1.062 | [0.500, 1.800] |
| $\sigma_{ka}$ | 0.7532 | N/A |
| $\sigma_{ke}$ | 0.2932 | N/A |
| $\sigma_c$ | 0.3539 | N/A |

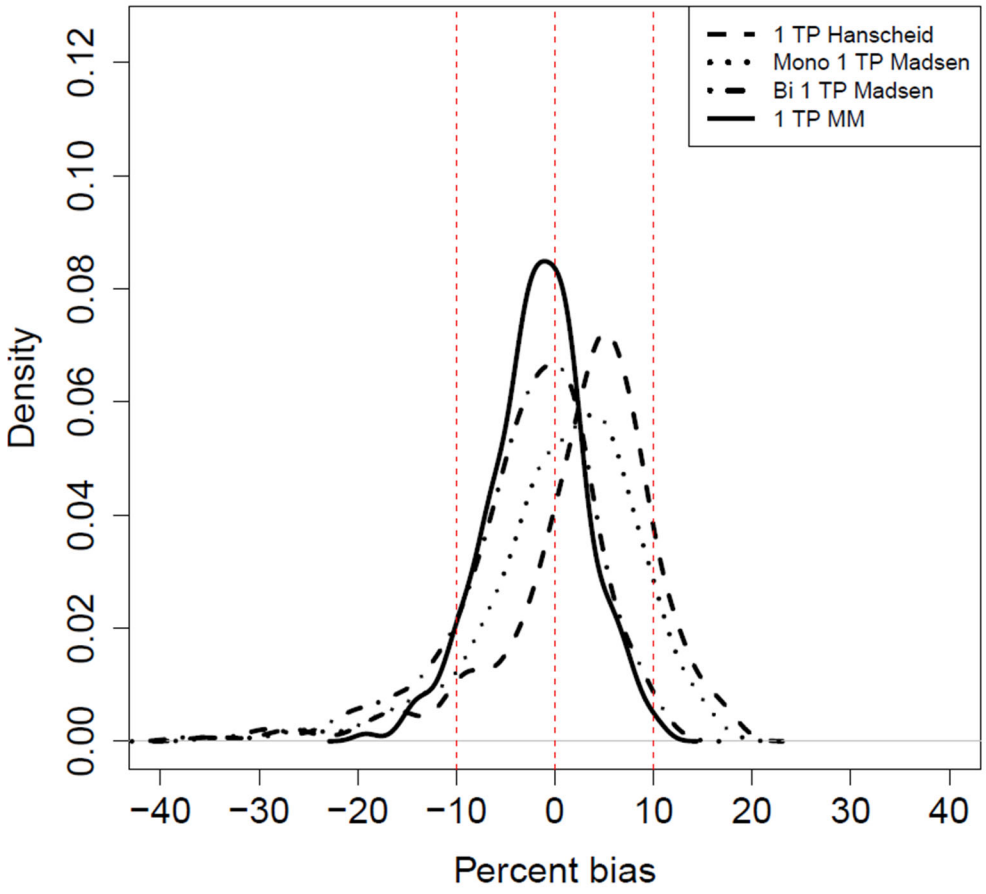


Supplemental Figure 1. Comparison of all single time point (TP) methods in terms of % bias in TIA in virtual cohort of 500 kidneys. MM = mixed model. “Mono” and “Bi” refer to monoexponential and biexponential fits, respectively.

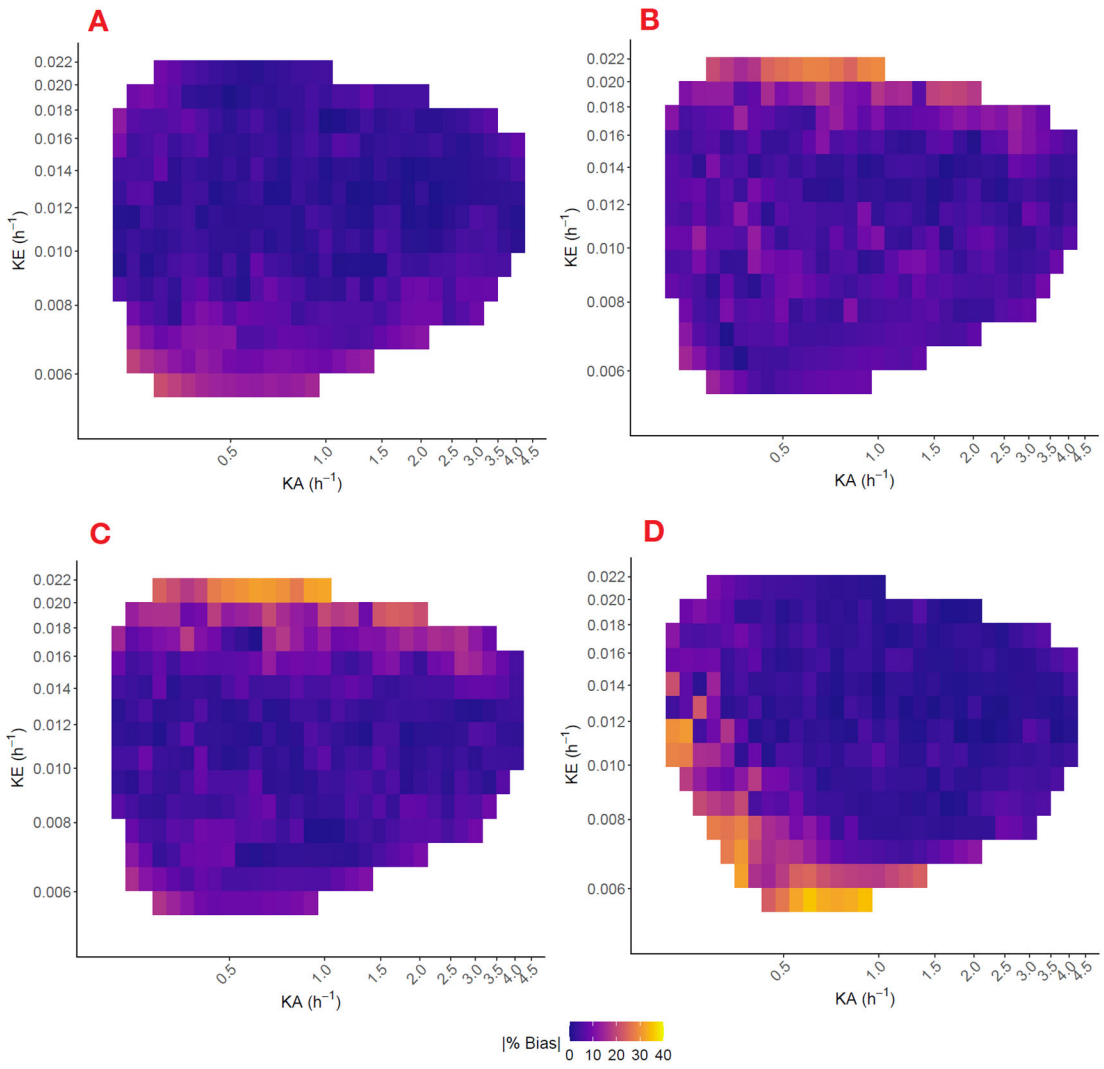


Supplemental Figure 2. Heat maps of |% bias| vs. biexponential parameters in 500 virtual kidneys for (A) two time point mixed model, (B) monoexponential Madsen method, (C) biexponential Madsen method, and (D) two time point monoexponential model. White space indicates regions where no kidneys with a specific combination of parameters were simulated. For visualization purposes, four kidneys with |% bias| > 100 were excluded from (D).

Graphical Abstract